THE PREDICTION OF VIBRATION, GROUNDBORNE AND STRUCTURE-RADIATED NOISE FROM RAILWAYS USING FINITE DIFFERENCE METHODS – PART I - THEORY

R M Thornely-Taylor   Rupert Taylor Ltd, Uckfield, East Sussex, TN22 3BG, UK

1   INTRODUCTION

The most accurate way of discovering the vibration, groundborne noise and structure-radiated noise generated by a railway is to construct it and measure the results. When it is necessary to know the results in advance, it is possible to model, numerically, the behaviour of the system and to "measure" the results in the model. The accuracy will depend of the appropriateness of the properties assigned to the elements of the model.

The finite-difference-time-domain (FDTD) method enables three-dimensional numerical modelling of a system with a moving source to be carried out efficiently. For radiation of noise through air to the far field, the FDTD method can be combined with the boundary element method enabling further computational efficiency.

2   THE FINITE DIFFERENCE ALGORITHM

2.1   Basic Principles

The wave equation in differential form is as follows

$$\mu\left(\frac{\partial^2 \xi}{\partial x^2} + \frac{\partial^2 \xi}{\partial y^2} + \frac{\partial^2 \xi}{\partial z^2}\right) + \left(\lambda + \mu\right)\left(\frac{\partial^2 \xi}{\partial x^2} + \frac{\partial^2 \eta}{\partial x \partial y} + \frac{\partial^2 \zeta}{\partial x \partial z}\right) = \rho \frac{\partial^2 \xi}{\partial t^2}$$

for the *x* axis, with corresponding equations for the *y* and *z* axes, where *x, y, z* and ξ, η and ζ are displacements in three orthogonal axes; λ and μ are Lamé constants and ρ is the density. The Lamé constant μ is also known as the shear modulus, *G*. The Lamé constant λ is also known as the coefficient of dilatation and is given by

$$\lambda = \frac{2\sigma G}{\left(1 - 2\sigma\right)}$$

where σ is Poisson's ratio.

The wave equation can be stated in finite difference form by replacing the differential operator with the approximation

$$\frac{\partial \xi}{\partial x} \approx (x[i][j][k] - x[i\text{-}1][j][k])/\Delta x$$

For $\Delta x \rightarrow 0$ these two forms are identical.

For a homogeneous, isotropic medium with a finite value for Δx, Δy and Δz, elastic wave propagation can be computed using the finite difference substitution

Effectively, the process is as follows, for each axis, i, j and k. The example given is for axis i. Each point p(i,j,k) lies at the corner of a rectangular cell and is assigned a mass equal to one eighth of the sum of the eight contiguous cells as well as a displacement and velocity. The displacement and velocity is interpolated for each intermediate "virtual" point p(i+d,i+d,k+d) where d=0 or 0.5.

1) Compute pressure gradient
2) Compute shear force gradient
3) Accelerate p(i,j,k) by $\Delta v = F/\rho \, \Delta t$ where F is the sum of the force 1 & 2 and ρ is the density assigned to the point and v is the point velocity.
4) Displace p(i,j,k) by $\Delta x = \Delta v * \Delta t$ where x is the point displacement and t is one time step.
5) repeat from step 1

The geometric part of wave propagation is completely represented by this process. However, it is not possible to compute force and velocity for the same cell element. Techniques are used to overcome this problem including the use of a staggered grid. For present purposes a process of interpolation to determine force and velocity at the same grid point is preferable. Cells are most conveniently rectangular, but other shapes are possible[12]

In principle the entire system can be represented by appropriate coding of cells to represent the vehicle body, suspension, bogies, wheels etc.

2.1.1 Wave types

Because of the general nature of the wave equation, provided that cells are coded appropriately, all wave types will emerge in an FDTD model provided that the wavelength is several times the individual cell size. Thus compression waves, shear waves, Rayleigh waves where there is a surface between the ground and an airspace or void, Stoneley waves at interfaces and Lamb waves in layers all occur where relevant without additional coding. In beams and plates, bending waves occur automatically and appropriate representation of supports produces correct beam and plate modes.

2.1.2 Damping

Damping can take several forms, including viscous, friction and hysteretic damping. In the finite difference algorithm is is possible to create a frequency dependent (including a frequency-independent) damping term with any desired spectrum shape using the relaxation principle of Boltzmann[3] where

$$s(t) = D_1\varepsilon(t) - \int_0^\infty \varepsilon(t - \Delta t)\varphi(\Delta t)d(\Delta t)$$

where $\varphi(\Delta t) = \dfrac{D_2}{\tau}e^{-\Delta t/\tau}$ is an after-effect function, D_2 is a constant and τ is a relaxation time. D_1 is a modulus, $s(t)$ is stress and $\varepsilon(t)$ is strain. By combining several after-effect functions with different values of D_2 and τ, any relationship between loss factor and frequency may be represented. Note that in the frequency domain the integral has a real and imaginary part, with the result that the value of the modulus is reduced by the inclusion of the relaxation terms. Depending on the choice of the constants and relaxation times, the stiffness of a resilient element will be frequency-dependent, and the value of D_1 must be adjusted at the same time that D_2 and τ are selected to give the required dynamic stiffness.

2.1.3   Model boundaries

The potential problem of spurious reflections from model boundaries can be overcome by the use of an impedance matching technique. This effectively assigns to the cells which are required to be non-reflective on the boundaries of the model the properties of a massless viscous damper such that

$$\frac{\eta K''}{\omega} = -\left(\rho c + \frac{D(\xi_o - \xi_{-1})}{\rho \Delta x v_0} \Delta t \right)$$

where η is the loss factor (dimensionless), K'' is the imaginary part of a complex spring stiffness in which the real part is zero, ω the angular frequency, ρc the characteristic impedance of the medium, ξ_0 and ξ_{-1} are the displacements of cell points 0 and -1 where the boundary is at cell 0, ρ is the density of the cell contents and v_0 is the velocity of cell 0.

2.1.4   Porous media and water saturation

The topic of sound propagation in fluid-saturated saturated porous solids was pioneered by Biot[45], Biot predicted the existence of two compressional waves and one shear wave. One of the compressional waves attenuates very rapidly, and the other can be regarded as a modified form of the compressional wave which would exist in the dry solid.

Biot's work was developed by Stoll[6] to include friction damping in the frame moduli, and was stated in generalised form by Yamamoto[7] as

$$\left.\begin{matrix} C_{p1} \\ C_{p2} \end{matrix}\right\} = \left[\left(\frac{2(HM - Q^2)}{(\rho M + m'H - 2\rho_f Q) \mp [(m'H - \rho M)^2 + 4\rho_f(\rho_f M - m'Q)H + 4\rho(m'Q - \rho_f M)Q]^{1/2}} \right) \right]^{1/2}$$

where the two complex roots yield values for the fast and slow compressional waves C_{p1} and C_{p2}. The imaginary part of a complex wave speed leads the loss factor through the relationship $\eta = 2$ x Im[$1/C^*$]/Re[$1/C^*$]. where C^* is a complex wave speed.

The Biot-Stoll shear wave velocity is given by

$$C_s = (\mu / \rho)^{1/2} (1 - \rho_f^2 / \rho m')^{-1/2}$$

H, Q and M are Biot's elastic moduli and related to the basic physical properties of porous media,

$$H = (K_r - K_s)^2/(D_r - K_s) + K_s + 4\mu/3$$
$$Q = K_r(K_r - K_s)/(D_r - K_s)$$
$$M = K_r^2/(D_r - K_s)$$
$$D_r = K_r[1 + \beta(K_r/K_f - 1)]$$

Where K_r is the bulk modulus of the frame material and K_f is the apparent bulk modulus of the pore fluid, and μ and K_s are the complex shear modulus and the complex bulk modulus of the skeletal frame, given by

$$\mu = \mu_r(1 + i\delta)$$

and

$$K_s = K_{sr}(1 + i\delta')$$

in which μ_r is the dynamic shear modulus, K_{sr} is the dynamic shear modulus, and δ *and* δ' are the loss factors of the skeletal frame. Also, ρ is the bulk density of the porous medium given by

$$\rho = (1-\beta)\rho_r + \beta\rho_f$$

where β is the porosity, ρ_r is the density of the frame material and ρ_f is the fluid density.

Finally, m' is the complex virtual mass density given by

$m' = (1 + \alpha)\rho_f/\beta - i[\eta F(\omega)/k_s\omega]$ in which α is the added mass coefficient of the frame (usually 0.25) and $F(\omega)$ is a viscous correction factor which, stated in terms of

$$\kappa = \frac{1}{7}d_{mean}\sqrt{\frac{\omega\rho_f}{\nu_f}}$$

as

$$F(\omega) = \frac{\kappa T}{4[1 + 2iT/\kappa]}$$

in which

$$T = \frac{ber'(\kappa) + ibei'(\kappa)}{ber(\kappa) + ibei(\kappa)}$$

where ber and bei are, respectively , the real and imaginary parts of the Kelvin fuction of the first kind or order zero, and ber' and bei' are their derivatives. The term ν_f is the fluid dynamic viscosity and d_{mean} is the mean grain size.

The Biot-Stoll formula gives a compressional wave which is always equal to or higher than the conventional elastic compression wave, and a second compressional wave which is slow and highly attenuated. While the second kind of wave can be ignored as a received signal, it is important in that a fractional of the initial wave energy is carried by it, and rapidly attenuated, reducing the amplitude of the fast wave, and also, on reflection at boundaries between soils of different impedances, some of the compression wave energy will be reflected as a wave of the slow kind, also to be rapidly attenuated. This may explain why field measurements of attenuation with distance from ground level or underground sources suggest higher loss factors than can be accounted for by friction, viscous or Masing effects.

By comparison, the Biot-Stoll formula for shear waves is more simply related to the classical shear wave speed for elastic media.

Stoll noted that when strain amplitudes are less than about 0.0001% soil moduli can be regarded as linear, and simpler equations for predicting velocity and attenuation are possible. He noted that in the case of dry materials such as sands, silts, sandstones and other granular materials, attenuation in low-amplitude waves may be adequately described by a model which assumes a constant loss factor. The principal mechanism of energy loss in these dry materials is friction that governs the minute amount of slip occurring within the contact area between particles. As a result the damping observed in a granular material is usually very small (e.g. typically of the order of 0.01 in sandstones and sands). When the pore spaces between the particles contain a fluid such as water, the observed attenuation is often significantly larger due to the addition of viscous losses in the fluid. In the case of materials with high permeability, there is overall motion of the fluid field relative to the skeletal frame. This result is frequency-dependent damping which changes rather rapidly over a fairly narrow frequency range. In finer materials with very low permeability, this kind of damping does not appear until quite high frequencies are reached. Another kind of viscous damping occurs, however, even in the low frequency range, as a result of local fluid motion in the vicinity of the intergranular contacts similar in nature to "squeeze film motion" as in the theory of lubrication. This second kind of viscous damping causes frequency dependent damping that can be described in terms of classical viscoelastic models.

The FDTD implementation of the Biot-Stoll equation can be simply achieved by using the equation to compute compressional wave speeds of the first kind, and shear wave speeds, and the frequency-dependent loss factor, and adjusting the parameters of the cells to yield the appropriate wave speeds and loss factors. Because the compressional wave of the second kind attenuates very rapidaly, it can be ignored. However, it does carry part of the vibrational energy, and at reflections between interfaces, for example at the top of a water table, some reflected energy will appear as a compressional wave of the second kind, to be rapidly attenuated. This is a form of damping which is not otherwise represented and may partially account for the higher observed attenuation rates than can be accounted for mathematically.

2.1.5 Non-linearity

Media such as soils exhibit non-linear properties. The give rise to strain-dependent moduli, and consequent damping. However, the effects ore only significant at strains larger than those normally encountered in non-seismic vibration propagation.

The non-linear behaviour of soil moduli was first expounded by Masing[8] Madshus[9] with reference to Isihara[10] gives the Masing rule as

In the loading half cycle:

$$\frac{T_a + T}{2} = T\left(\frac{\Gamma_a + \Gamma}{2}\right)$$

In the unloading half cycle:

$$\frac{T_a - T}{2} = T\left(\frac{\Gamma_a - \Gamma}{2}\right)$$

where the brackets signify that T is a function of Γ as follows according to the hyperbolic soil model of Hardin and Drnevich[11]

$$T(\Gamma) = G_{max} \cdot \frac{\Gamma}{1 + \dfrac{\Gamma}{\Gamma_r}}$$

G_{max} is the shear modulus for infinitesimally small strains; Γ is strain, and

$$\Gamma_r = \frac{T_f}{G_{max}}$$

where T_f is the shear strength

The formula for the damping which results from the non-linear stress-strain relationship is

$$D_H = \frac{4}{\pi}\left(1 + \frac{\Gamma_r}{\Gamma_a}\right)\left(1 - \frac{\Gamma_r}{\Gamma_a} \bullet \ln\left(1 + \frac{\Gamma_a}{\Gamma_r}\right)\right) - \frac{2}{\pi}$$

2.1.6 Anisotropy

Many soils, particularly overconsolidated clays, have moduli which depend on direction. A particular advantage of the FDTD method is that difference values of G and D can be applied to the I, j and k directions. The dependence of moduli on confining pressure, and thereby on depth below ground can also be taken into account by varying the values of G and D with increasing depth.

2.1.7 Stability

For a FDTD model to be stable, the time step used must not exceed the Courant number, given by

$$\Delta t \leq \frac{1}{c\sqrt{\frac{1}{\Delta x^2} + \frac{1}{\Delta y^2} + \frac{1}{\Delta z^2}}}$$

where Δx, Δy, and Δz are the cell sizes in the I, j and k directions.

2.1.8 Bandwidth

The lower limit of the bandwidth of an FDTD model is dependent on the run time, which should preferably be at least $4/f_o$ where f_o is the lower boundary of the frequency range. The upper limit is defined by the cell size, and the must be at least two cells per wavelength, and preferably four or more cells per wavelength. The input forcing signal should be filtered with a cut-off at the upper frequency limit of the bandwidth.

2.1.9 Excitation and input force

For a railway model, the excitation should be, firstly, a time-dependent force caused by the wheel/rail roughness profile. This is input as the force caused by the displacement of the Hertzian contact spring between a railway wheel and the rail, typically assumed to be 1.2 GN/m. However, the train is moving, so the point of contact must move at the same rate. To avoid a step-wise motion, the application of the force to the rail is preferably achieved by polynomial interpolation across the edges of adjacent cells. Secondly, the effect of the moving load at the wheel is modelled by applying the acceleration due to gravity to the wheel at each time step.

The wheel/rail roughness profile may be an actual profile measured from actual track,. Or a synthesised profile which has the amplitude and spectrum shape typically found on the type of railway in question. Joints in the rail or flat spots on the wheel tread can be introduced as superimposed displacements in the roughness signal.

3   THE BOUNDARY ELEMENT ALGORITHM

For the prediction of noise from a vibration structure such as a railway viaduct, in the far field, it is possible to extend the FDTD grid to a large enough size to include the receptor locations. However, a smaller grid can be used, and computation time saved, by using a boundary element technique to predict sound pressure levels in the far field. The FDTD part of the model is used to compute the velocity and pressure on the face of each cell representing the structure, for input to the boundary element model.

The boundary integral equation in the frequency domain[12] is

$$4\pi p(P) = -\int_s [p(Q)G'(Q,P) + ik_o v_n(Q)G(Q,P)]dS(Q)$$

Where $p(P)$ is the sound pressure at a point P, $p(Q)$ and $v_n(Q)$ are the sound pressure and normal velocity distributions on the surface of the body, k_o is the wave number and Q is a point on the surface of the radiating body. G is the free-field Green's function $G(Q,P) = e^{-ikr}/r$, where $r = |Q-P|$, the distance between points Q and P, and G' is the derivative of G in the direction normal to the body. Effectively the equation states that the sound pressure at any point P is composed on the sum of the contributions of a dipole distribution of surface pressure and a monopole distribution of surface acceleration. The FD module computes both the sound pressure and acceleration at each radiating element, and computes the contributions of each element at each receptor for each time step.

4   CHOOSING CELL PROPERTIES

The accuracy of an FDTD model depends of course on the appropriate assignment of properties to each cell. The properties to be assigned are shear modulus, compression modulus, (or shear modulus and Poisson's ratio), loss factor and density. Loss factor is likely to be frequency dependent, and the use of the Boltzmann relaxation method produces some frequency dependence in the moduli, with the result that the Boltzmann parameters must be chosen not only to give the appropriate loss factor, but also the appropriate shear and compression moduli all as a function of frequency.

Because of the limitations of the Courant number, very small cell sizes, for example to represent the webs and flanges of steel beams, can lead to excessively short timesteps and excessive run times. This problem can be overcome by representing an element such as an "H" section beam as a rectangular bar, and assigning sizes for Δx, Δy and Δz, and for shear and compression modulus, to give the same value of bending stiffness in each direction, and mass per unit length, as those possessed by the actual section. Bending stiffness is the product of Young's modulus and the second moment of area of the section. This simplification is acceptable when the only significant contribution of the element is in terms of bending waves. In cases where longitudinal wave propagation along the beam is significant, its true moduli and cross section must be used.

For concrete structures, a decision has to be made on whether to assume the long-term or short-term Young's modulus, and the normal approach is to assume short-term values.

For soils and rocks, moduli for infinitesimally small strains must be used, which effectively means that data from measurements of wave speeds, rather than from direct measurements of moduli are required, and these must be adjusted for the effect of confining pressure, and depth below ground. Where appropriate anisotropic material such as clay may require different moduli for each direction. The presence of a water table must be taken into account by using appropriate saturated and unsaturated values for D.

When a model includes an airspace, for example air in a room, and sound pressure levels are to be computed, the effect of sound absorption in the room must be taken into account. This can be simplified if the reverberation time of the room is known or can be reliably assumed, and the effect of absorbent room surfaces taken into account by artificially increasing air absorption, giving air a loss factor of

$$\eta \approx \frac{4.4}{f \, T_{60}}$$

where f is frequency in Hz.

5   MODEL VERIFICATION AND VALIDATION

Model verification is carried out by running models of structures and cases for which algebraic solutions are available, including propagation of compression, shear and other wave types in bounded, unbounded and layered media, and plates and beams. The effect of errors in cell property assumptions requires studies of the effects and probabilities of variations in cell properties.

Model validation against field measurements clearly requires accurate knowledge of the material properties in the field case. The topics of calibration, validation and verification are addressed in Appendix C of reference 13.

6   MODEL EXAMPLES

Examples of FDTD models are given in Figures 1 to 6 below, including instanteous cross sections showing the displacements of cells. Because the displacement of rails is large compared with displacements of structural elements and surrounding soil, rail displacements have been suppressed in the cross sections and the displacements of the surrounding elements greatly exaggerated in order to display them clearly.
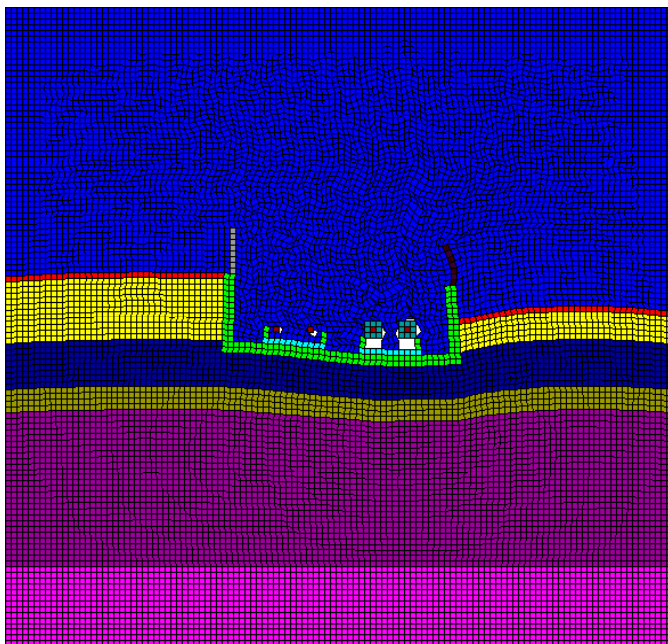

Figure 1 Instantaneous cross section through model of railway in concrete trough (rail displacement suppressed)
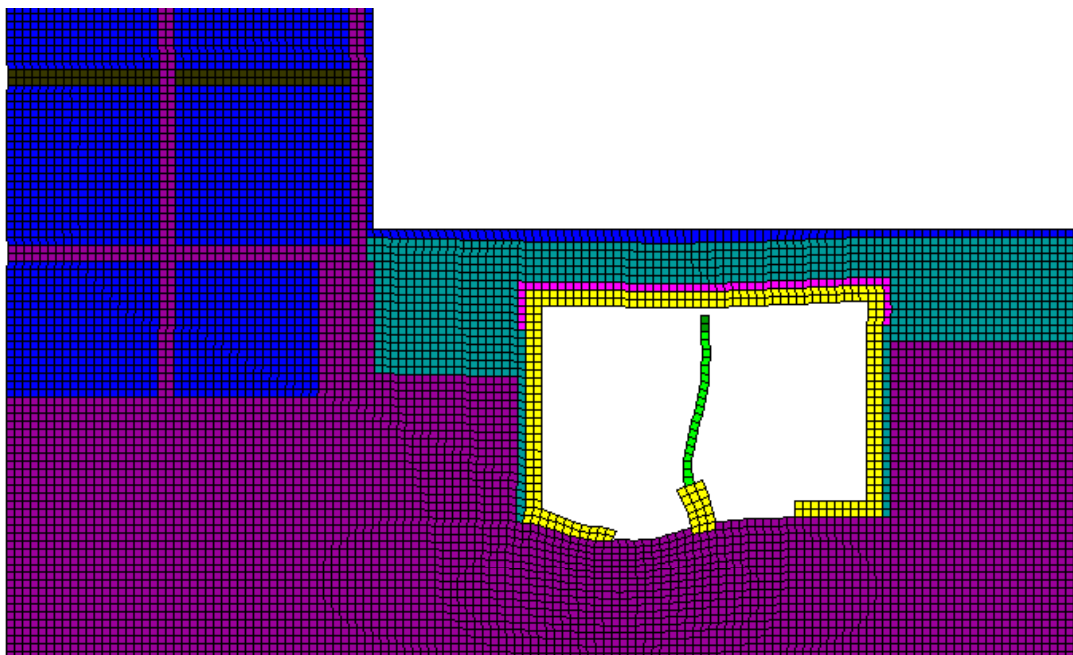
Figure 2 Instantaneous cross section through model of railway iin cut and cover tunnel adjacent to building (rails, sleepers and ballast omitted for clarity)
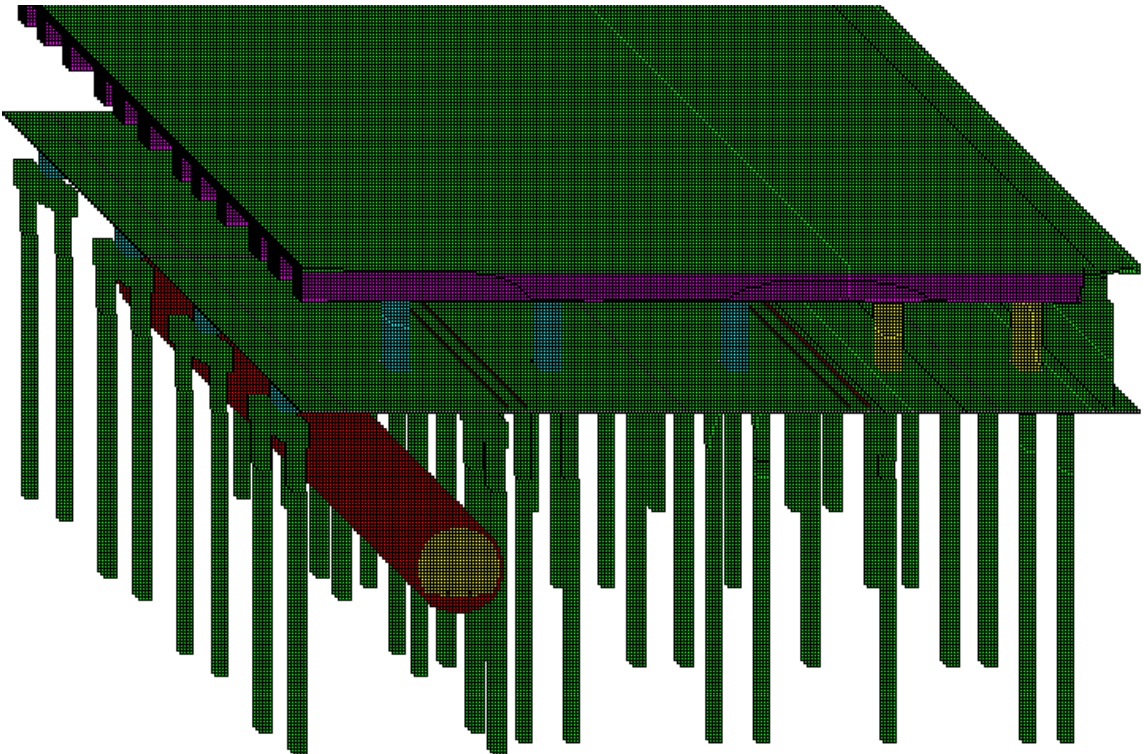
Figure 3 Isometric view of model of railway depot building on piled foundations above bored railway tunnel (soil around piles omitted for clarity)
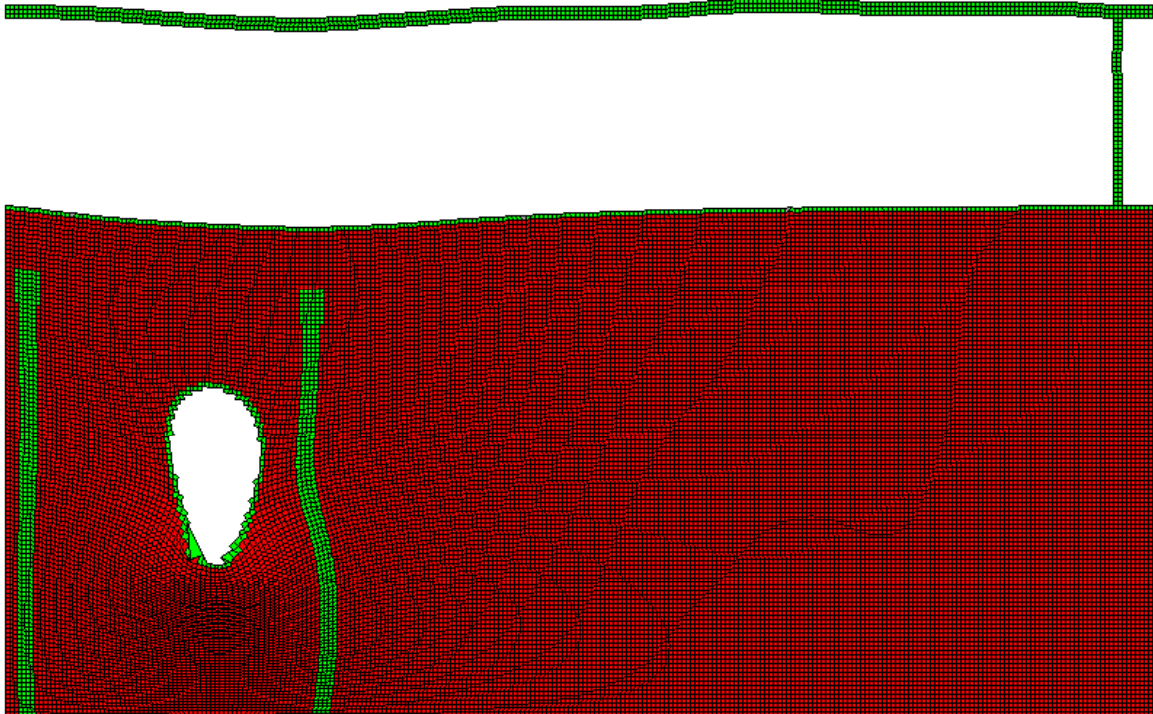

Figure 4 Instantaneous cross section through building in Figure 3 (rails omitted for clarity)
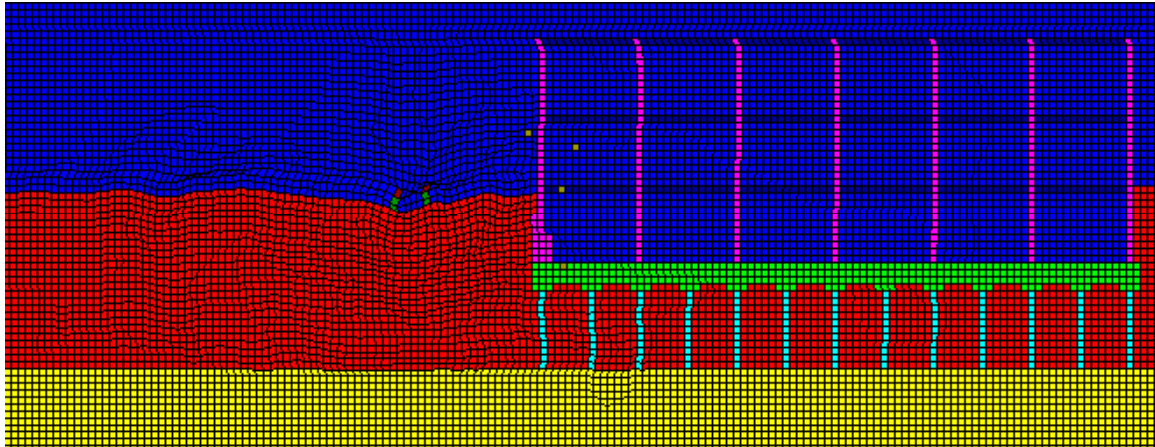
Figure 5 Instantaneous cross section through model of street-running tram adjacent to building founded on piles bearing on rock.
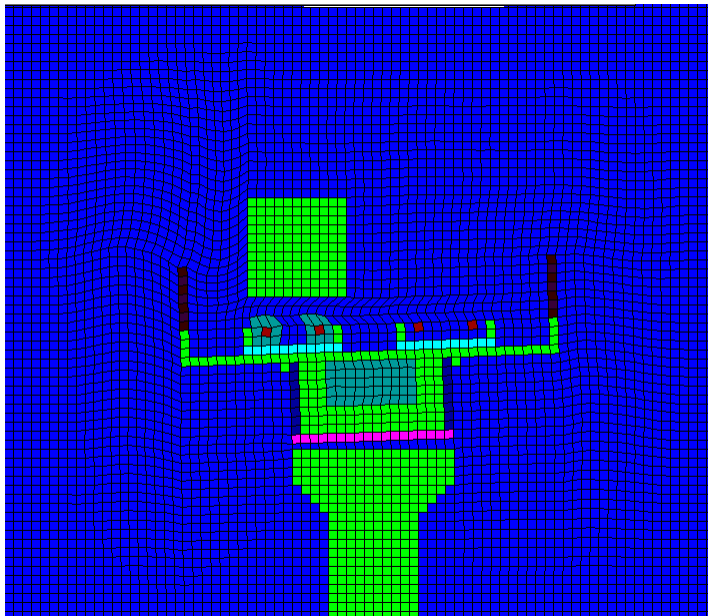

Figure 6. Instantaneous cross section through railway on viaduct

Output from the model is initially in the form of a time domain plot of, for the case of vibration, the displacement, velocity or acceleration, and in the case of airborne noise the sound pressure. Plots of this kind may be produced for all ro any cells in the model, the only cost being consumption of hard disk space and the large quantity of results.

The time domain plot may be converted to a .WAV file and replayed through loudspeakers if required for auralisation purposes. Otherwise it may be subjected to frequency transformation into either narrow band spectra or 1/3 octave frequency bands.

The vibration acceleration signal may be subjected to frequency weighting and the fourth-power integral obtained to give Vibration Dose Value. The airborne noise signal may be A-weighted and the square of the signal integrated in order to yield L_{AE} (SEL) and thereby compute L_{Aeq} levels.

Examples of time-domain, narrow band and 1/3 octave band spectra are shown in figures 7 to 9. The time-domain output may also be converted to a WAV file for auralisation.
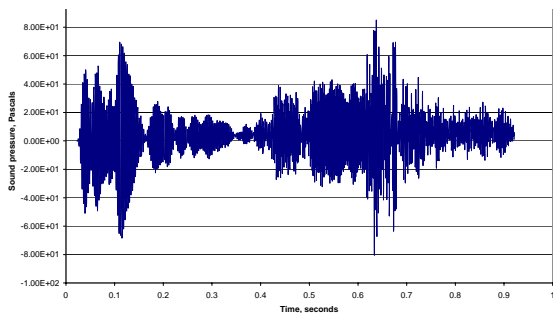
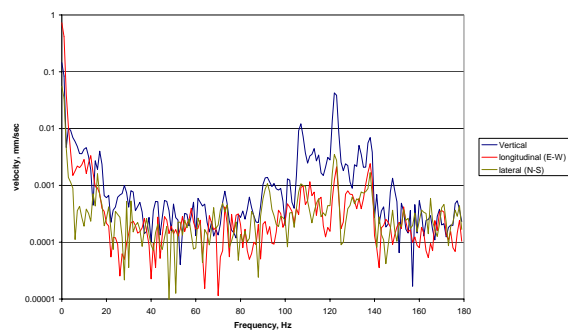Figure 7   Example of Time-domain output
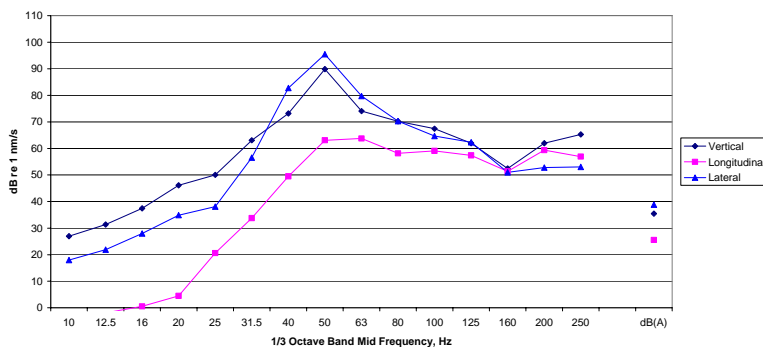

Figure 8   Example of narrow band output

Figure 9   Example of 1/3 octave band output

7   REFERENCES

[1] Botteldooren, D, Acoustical finite-differense time-domain simulation in a quasi-Cartestian grid, J. Acoustic.Soc. Am. 95(5) Pt 1, May 1994.

[2] Tolan, J.G. and Schneider, J.B. Locally conformal method for acoustic finite-difference time-domain modeling of rigid surfaces, J. Acoustic. Soc. Am. 114 (5) November 2003

[3] Boltzmann. L. Ann. Physik, Erg. Bd. 7 (1876) 624-654

[4] Biot, M.A. Theory of Propagation of Elastic Waves in a Fluid-Saturated Poroud Solid – I Low Frequency Range Frequency Rage, J. Acoustc. Soc. Am. 28, 2 1956

[5] Biot, M.A. Theory of Propagation of Elastic Waves in a Fluid-Saturated Poroud Solid – II Higher Frequency Range, J. Acoustc. Soc. Am. 28, 2 1956

[6] Stoll, R.D., Marine Sediment Acoustics, J. Acoust. Soc. Am 77 (5) May 1985

[7] Yamamoto, T. and Turgut, A. Acoustic wave propagation through porous media with arbitrary pore size distributions, J. Acoust. Soc. Am. 83(5), May 1988

[8] Masing, G, Eigenspannungen und Verfestigung beim Messing. Proc.: 2nd International Congress for Applied Mechanics, Zurich, 1928, pp.332-335

[9] Madshus, C, Soil Non-linearity and its Effect on the Dynamic Behaviour of Offshore Platform Foundations, D.Sc Dissertation, Department of Geology, Faculty of Mathematics and Natural Sciences, University of Oslo

[10] Isihara. K. Evaluation of Soil Properties for use in Earthquake Response Analysis. Proc.: Int. Symposium on Numerical Models in Geomechanics, Zurich, 13-17 September 1982.

[11] Hardin. B.O. and Drnevich, V.P. Shear Modulus and Damping of Soils, Design Equations and Curves, Proc., ASCE, Vol 98, SM7, pp. 667-692

[12] Seybert, A.F. and Wu, T.W. Acoustic Modeling: Boundary Element Methods, in Encyclopaedia of Acoustics, Crocker, M.J. ed.

[13] Mechanical vibration — Groundborne noise and vibration arising from rail systems — Part 1: General Guidance, ISO/DIS 14835-1, International Standards Organization